

# 1    Regionalized life-cycle water impacts of microalgal- 2    based biofuels in the US

3    *David Quiroz<sup>a</sup>, Jonah M. Greene<sup>a</sup>, Jason C. Quinn<sup>a\*</sup>*

4    <sup>a</sup>Mechanical Engineering Department, Colorado State University, 1374 Campus Delivery, Fort  
5    Collins, Colorado 80522, United States

6    \*Email: jason.quinn@colostate.edu

7    KEYWORDS. Algae, bioenergy, water footprint, water scarcity footprint, life-cycle assessment

8    ABSTRACT. While algal biofuels have the potential to reduce the national reliance on fossil fuels,  
9    the high water consumption associated with algal biomass cultivation represents a major concern  
10    compromising the sustainable commercialization of this technology. This study focuses on  
11    quantifying the water footprint (WF) and water scarcity footprint (WSF) of renewable diesel  
12    derived from algal biomass and provides insights into where algal cultivation is less water-  
13    intensive than traditional ethanol and biodiesel feedstocks. Results are generated with an  
14    engineering process model developed to predict the life cycle water consumption, considering  
15    green, blue, and gray water, of algae facilities across the United States at a high spatiotemporal  
16    resolution. The model predicts average blue WFs of 1.6 and 14.9 m<sup>3</sup> GJ<sup>-1</sup> in Florida and Arizona,  
17    respectively. When total WFs are compared, the total WF in Arizona is 26% larger than that of  
18    Florida, with dramatic differences between blue and green WFs locations. The analysis reveals

19 that the total life cycle WFs of algal renewable diesel are smaller than the optimal WFs of corn  
20 ethanol and soybean biodiesel. Algal systems benefit from higher growth rates and offer the  
21 opportunity to manage wastewater streams, therefore generating smaller green and gray WFs than  
22 those of conventional biofuels. The WSF analysis identifies the Gulf Coast as the most suitable  
23 region for algal cultivation, with cultivation in the western US shown to exacerbate local water  
24 stress levels.

25

## 26 **1. Introduction**

27 Microalgae-derived fuels are perceived as promising alternatives to decarbonizing the  
28 transportation sector. As a third-generation biofuel, cultivation of algal biomass does not  
29 compromise food security and multiple algae species possess higher photosynthetic efficiencies  
30 and generate greater oil yields than terrestrial energy crops <sup>1,2</sup>. In addition, algae-to-fuel  
31 pathways have the potential to generate a variety of high-value co-products, which could  
32 potentially improve the economics of algae systems, while concurrently reducing greenhouse gas  
33 emissions <sup>3</sup>. However, additional research and development are required not only to reach  
34 economic parity with conventional fuels but also to understand the local and regional  
35 environmental impacts of commercial-scale algal biofuel production.<sup>3</sup>

36 Although there are multiple life-cycle assessments (LCA) focused on algal biofuels in the  
37 literature, the lack of freshwater consumption impacts represents a major research gap in the  
38 field.<sup>3</sup> Understanding the added water demand that algal cultivation will have on local water  
39 sources is paramount to avoid future water-related risks, particularly when the cultivation of  
40 algal biomass is envisioned to be deployed in locations that are experiencing considerable water  
41 shortages such as the southwest United States (US).<sup>4</sup> Water consumption is often measured using

42 a water footprint (WF) methodology, where the WF of a product is the sum of direct and indirect  
43 water consumption.<sup>5</sup> More recently, a new method to assess the water scarcity footprint (WSF)  
44 of a product has been proposed by the Water Use in LCA (WULCA) research group.<sup>6</sup> The  
45 Available Water Remaining (AWARE) is a consensus-based model used to determine a WSF  
46 based on a characterization factor that quantifies water availability and demand in a specific  
47 region over a set timeframe.<sup>7</sup>

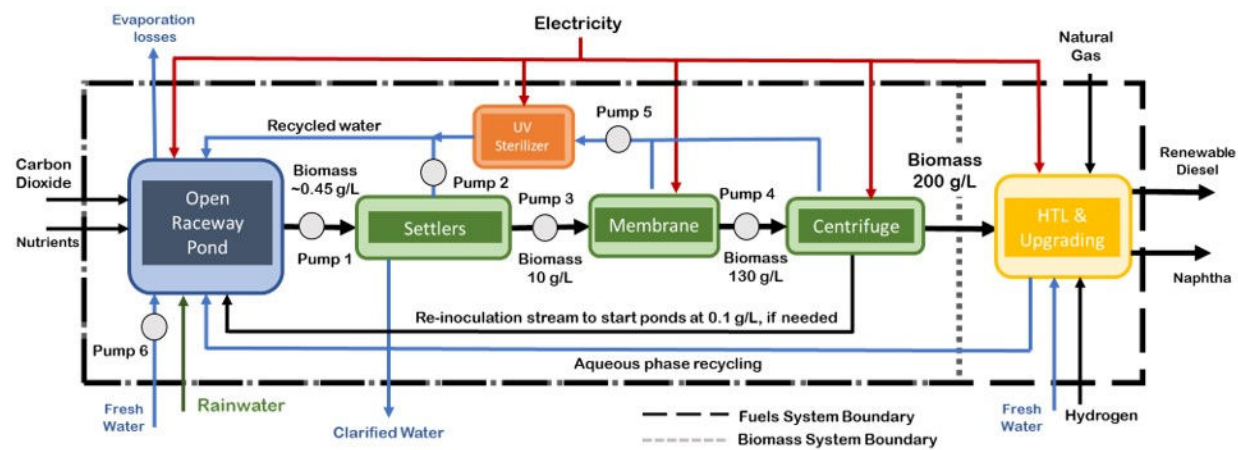
48 In previous assessments, the water consumption of algal systems has been estimated using the  
49 discussed methods. However, studies often employed one method exclusively resulting in either  
50 a WF<sup>8-13</sup> or WSF accounting<sup>14,1</sup> and fail to provide a complete assessment of the water impacts.  
51 Previous studies do not account for geographic considerations or are restricted to a few  
52 locations.<sup>8,10,13,16</sup> In addition, multiple studies do not use a life-cycle assessment framework and  
53 neglect water consumption of upstream processes or the direct consumption of the conversion to  
54 fuel process<sup>8,11,14,17</sup>, which underestimates the total water consumption of the algae to fuels  
55 process.<sup>10,18</sup> More importantly, quantifying the contribution of rainwater to the water footprint of  
56 algal systems is important to make an objective comparison to terrestrial crops. An accurate  
57 water balance requires models able to calculate evaporation rates at a high spatiotemporal scale<sup>11</sup>  
58 and careful tracking of algal pond depth to avoid culture dilution caused by high precipitation  
59 rates.<sup>8</sup> Wigmosta et al.<sup>17</sup> is the only study that includes rainwater in water balance calculations,  
60 however, the evaporation model used in the analysis was validated with small-scale pond data  
61 and was not designed to estimate the evaporation rates of commercial-scale systems accurately.<sup>11</sup>  
62 This is critical as evaporation rates not only impact water balances but also propagate to  
63 temperature and growth rate calculations.<sup>11</sup> The WF of algal systems has not been clearly defined

64 in the literature due to a lack of appropriate models and incorrect modeling assumptions or  
65 methodological inconsistencies.

66 This study focuses on estimating the WF and WSF of renewable diesel derived from algal  
67 biomass by integrating water life cycle assessment methodologies with a robust dynamic  
68 cultivation model. This work builds upon previous modeling work<sup>11</sup> with novel aspects including  
69 a thorough investigation of the impacts of water recycling, rainwater, and indirect water  
70 consumption on the WF of the system. By using the high-fidelity model validated by Quiroz et  
71 al.<sup>11</sup>, the impacts of system scale on evaporation rates and consequently on water consumption,  
72 pond temperatures, and growth rates are accurately modeled. In addition, ~~Results from the model~~  
73 ~~provide freshwater and rainwater consumption of the biomass production process with a high~~  
74 ~~spatial and temporal resolution that is. Furthermore,~~ the cultivation model was coupled with a  
75 state-of-the-art conversion model<sup>19</sup> to analyze the direct and indirect water consumption of the  
76 biomass-to-fuel process. The local water scarcity impacts associated with the deployment of  
77 commercial-scale algal biofuel systems across the US are also investigated. When integrated, the  
78 models provide a geospatial analysis of the life cycle WF, including blue, green, and indirect  
79 WFs, and WSF of the algae to renewable diesel process. Results identify the most water-  
80 intensive processes in the algae-to-fuel pathway, compare the magnitudes of direct and indirect  
81 water consumption, and illustrate the most suitable locations for algae fuel production based on  
82 water consumption impacts. The discussion focuses on comparing these results to the water  
83 intensity of saline algal cultivation and traditional biofuel systems. ~~feedstocks and biofuels.~~ This  
84 is the first work to complete a holistic life cycle water assessment and water scarcity evaluation  
85 for the entire US of an algal-based biorefinery.

86 **2. Methods**

87 This study assesses the geographically resolved water consumption of algal biofuels through  
88 two different water LCA methodologies. Both are informed by mass and energy balances  
89 calculated from an engineering process model encompassing the geographically resolved  
90 biomass cultivation, dewatering, and fuel conversion stages, as shown in Figure 1. The following  
91 subsections provide detailed descriptions of the cultivation (including the growth model),  
92 conversion, and water LCA methods adopted in this study.



94 **Figure 1.** System diagram illustrating the microalgae cultivation process in open-raceway ponds,  
95 three-step dewatering process, and conversion and upgrading to renewable diesel through  
96 hydrothermal liquefaction (HTL) and hydrocracking.

97 **2.1 Cultivation Model**

98 The cultivation model used in this analysis includes the biomass growth process in  
99 commercial-scale open-raceway pond (ORP) systems followed by a three-step dewatering  
100 process consisting of settlers, membranes, and centrifuges. Detailed descriptions of these  
101 modules are provided in the following subsections.

102 **2.1.1 Open-Raceway Pond Model**

103 ORPs have been the most studied algae growth architecture in the literature due to their low  
104 cost and simplicity. Given the open nature of these systems, ORPs are subjected to the changing

105 conditions of the environment, therefore, models with hourly timescales are required to  
106 accurately simulate pond conditions. Thermal conditions in the ORP system were calculated  
107 using the model validated by Quiroz et al.<sup>11</sup>, while growth rates were simulated using the  
108 dynamic growth model validated by Greene et al.<sup>20</sup> Temporally and spatially resolved outputs for  
109 a 400-hectare facility cultivating the strain UTEX 393 were generated following the framework  
110 in previous modeling work with results presented in the Supporting Information (SI).<sup>11</sup>

111 The foundational model from Quiroz et al.<sup>11</sup> was modified to include precipitation data to  
112 model realistic pond operations. Daily precipitation data for 21 years, retrieved from the Center  
113 for Hydrometeorology and Remote Sensing database, was disaggregated into hourly time steps  
114 and included in the water balance.<sup>21</sup> The depth of the ponds was kept between 15 and 25 cm by  
115 tracking hourly net evaporation rates, defined as the difference between evaporation and  
116 precipitation rates. If the pond depth exceeded the allowable maximum, the pond was harvested  
117 and reset to 15 cm and a concentration of  $0.1 \text{ g L}^{-1}$ . Similarly, potential culture dilution caused by  
118 incoming precipitation was prevented by ensuring the concentration in the ponds was maintained  
119 above  $0.1 \text{ g L}^{-1}$ . Further details on model calculations, implementation, and data curation are  
120 presented in the SI.

121 **2.1.2 Dewatering Model**

122 The dewatering module is composed of a three-step dewatering process to remove excess  
123 water from the biomass,  $0.45 \text{ g L}^{-1}$  to  $200 \text{ g L}^{-1}$ , based on the modeling work of Davis et al.<sup>22</sup> The  
124 biomass was first routed through settlers where it exits with a concentration of  $10 \text{ g L}^{-1}$ . The  
125 water retrieved from the biomass stream is recycled back to the ponds except for when the ponds  
126 are drained due to excess precipitation. During pond drainage, the clarified water was routed  
127 back to the local water source. The clarified water stream exiting the settlers was assumed to  
128 contain a negligible concentration of nutrients and algae.<sup>22</sup>

129 Subsequently, the biomass stream is routed to the remaining dewatering processes depicted in  
130 **Error! Reference source not found.**, and recycled water is sterilized in an ultra-violet sterilizer  
131 before being returned to the ORPs. For the case when ponds do not have enough biomass to be  
132 restarted to  $0.1 \text{ g L}^{-1}$ , mainly caused by constant harvesting during intense precipitation periods,  
133 a fraction of biomass is routed from the exit stream of the centrifuge back to the ponds. This  
134 pond operating strategy reduces freshwater consumption by storing all available rainfall and  
135 preventing culture failure induced by diluted cultures.

136 Energetics and recycling efficiencies of the dewatering and cultivation equipment are  
137 presented in Table 1. The recycling efficiencies used in this study are informed by previous  
138 modeling work in the literature<sup>22</sup> and represent a current technical hurdle that must be addressed  
139 for the optimal performance of commercial-scale systems. The impacts of these assumptions and  
140 other key model inputs were tested through a sensitivity analysis, and further methods are  
141 presented in the SI.

142

143

144

145

146

147

148

149

150

151

152 **Table 1.** Primary model inputs used for the calculation of mass and energy flows in the biomass  
 153 production process.

	Value	Unit
<b>Open-Raceway Ponds</b>		
Inoculation density <sup>11</sup>	100	g L <sup>-1</sup>
Harvest density <sup>11</sup>	450	g L <sup>-1</sup>
Harvest volume <sup>23</sup>	75	%, fraction of pond
CO <sub>2</sub> utilization <sup>22</sup>	90	%
<b>Biomass Elemental Composition</b>		
Carbon (C) <sup>22</sup>	48.3	%, AFDW basis
Nitrogen (N) <sup>22</sup>	9.5	%, AFDW basis
Phosphorous (N) <sup>22</sup>	1.2	%, AFDW basis
Others (H, O, S) <sup>22</sup>	41.0	%, AFDW basis
<b>Biomass Component Composition</b>		
Lipids <sup>22</sup>	22.1	%, AFDW basis
Protein <sup>22</sup>	25.4	%, AFDW basis
Carbohydrates <sup>22</sup>	52.5	%, AFDW basis
Ash <sup>22</sup>	8.00	%, DW basis
<b>Diammonium Phosphate Composition</b>		
Phosphorous <sup>20</sup>	20	%, weight
Nitrogen <sup>20</sup>	18	%, weight
<b>Ammonia Composition</b>		
Nitrogen <sup>20</sup>	82	%, weight
<b>Dewatering</b>		
Settlers target concentration <sup>22</sup>	10	g L <sup>-1</sup>
Biomass blowdown loss <sup>22</sup>	0.1	%
Settlers separation efficiency <sup>22</sup>	90	%
Membrane target concentration <sup>22</sup>	130	g L <sup>-1</sup>
Membrane separation efficiency <sup>22</sup>	99.5	%
Centrifuge target concentration <sup>22</sup>	200	g L <sup>-1</sup>
Centrifuge separation efficiency <sup>22</sup>	97	%
<b>Energy Consumption</b>		
CO <sub>2</sub> delivery power <sup>22</sup>	0.0439	kWh kg <sup>-1</sup> CO <sub>2</sub>
Paddlewheel power <sup>22</sup>	55.1	kWh hectare <sup>-1</sup> day <sup>-1</sup>
Membrane power <sup>22</sup>	0.04	kWh m <sup>-3</sup>
Centrifuge power <sup>22</sup>	1.35	kWh m <sup>-3</sup>
UV sterilizer power <sup>22</sup>	2.71e-03	kWh m <sup>-3</sup>
Freshwater pump power <sup>22</sup>	0.257	kWh m <sup>-3</sup>
Ponds to settlers pump power <sup>22</sup>	0.0189	kWh m <sup>-3</sup>
Settlers recycling pump power <sup>22</sup>	0.0177	kWh m <sup>-3</sup>
Settlers to membrane pump power <sup>22</sup>	0.129	kWh m <sup>-3</sup>
Membrane to centrifuge pump power <sup>22</sup>	0.0194	kWh m <sup>-3</sup>
Recycling stream pump power <sup>22</sup>	0.184	kWh m <sup>-3</sup>

154

155

156 **2.2 Conversion Model**

157 After dewatering the biomass to 20% solids, the biomass was converted to biocrude via  
158 hydrothermal liquefaction (HTL) based on the work of Chen et al.<sup>19</sup> Inputs to the HTL model  
159 include biomass composition and biomass productivity yields. The ash-free lipid, protein, and  
160 carbohydrate content of the biomass were set to 22%, 25%, and 53%, respectively.<sup>23</sup> The ash  
161 content of the biomass was assumed to be 8%.<sup>23</sup> After the biomass is processed to a biocrude,  
162 upgrading to renewable diesel and naphtha is done via hydrocracking.<sup>19</sup> The nutrient-rich  
163 aqueous stream exiting the HTL module is recycled back to the ponds, while the gaseous stream  
164 is utilized for on-site heat and power.<sup>19</sup>

165 **2.3 Water LCA Methods**

166 The primary goal of this study is to determine the WF and WSF of microalgae biomass and  
167 biofuels. The direct and indirect water consumption of the supply chain was included to provide  
168 a final value of life cycle water consumed per functional unit. Two different system boundaries  
169 were established to facilitate comparison to other energy crops and biofuels from previous  
170 assessments. The first system boundary includes the biomass cultivation and dewatering to 20%  
171 solids processes while the second system boundary is expanded to incorporate the fuel  
172 conversion process (Fig. 1). Similarly, the functional units for each system configuration were  
173 set to one metric ton of ash-free dry weight biomass and one GJ of renewable diesel,  
174 respectively.

175 **2.3.1 Water Footprint Methodology**

176 The most common method used to quantify the water consumption of bioenergy systems is the  
177 water footprint method developed by Hoekstra et al.<sup>5</sup> The total WF of a product is defined as the  
178 addition of three different WF components: blue, green, and gray WFs. Each component is  
179 further divided into a direct and indirect WF. The indirect WF measures upstream water  
180 consumption in the supply chain, while the direct WF refers to on-site water consumption. It is

181 worth noting that this method considers water consumption only and neglects the impacts to  
182 water quality.<sup>5</sup>

183 The blue WF of a product measures the amount of water consumed from surface or  
184 groundwater sources.<sup>5</sup> In the case of algal cultivation, freshwater consumption is equal to the  
185 difference between the volume of water withdrawn from the water source (to make up for  
186 evaporation losses and water incorporated in the biomass stream) and the volume of clarified  
187 water returned to the catchment area, due to system drainage. Accordingly, an increase in the  
188 water discharged due to inefficiencies in the dewatering equipment has no impact on the net  
189 freshwater consumption of the system. However, an increment in the volume of discharged water  
190 could have implications for the gray WF of the system, as discussed below. The water used for  
191 cooling equipment and other processes in the conversion stage was assumed to all be consumed,  
192 making the total blue water demand equal to the sum of the water consumed in the cultivation  
193 and conversion processes.

194 In addition to estimating blue WFs, computing the green WF is essential in the water analysis  
195 of energy crops. The green WF measures the volume of rainfall that is not returned to  
196 groundwater sources and is either stored or consumed.<sup>5</sup> Green water demand was calculated by  
197 tracking the volume of rain entering the ponds. This study assumed that all rainwater is stored in  
198 the ponds and therefore all precipitation contributes to the green WF.

199 In contrast to the blue and green components, the gray WF measures freshwater pollution and  
200 is defined as the volume of freshwater required to dilute pollutants to meet water quality  
201 standards.<sup>5</sup> Different from terrestrial crops, the gray WF of algal cultivation can be minimized  
202 by proper nutrient recycling and treating waste streams before disposal.<sup>16</sup> For example, all  
203 disposed water from cultivation is previously clarified in the settlers to reduce the concentration

204 of suspended solids in the clarified water stream. Based on experimental data reported in the  
205 literature<sup>24-27</sup>, the algae culture was assumed to consume all available nutrients and therefore the  
206 nutrient load in the harvested and water discharged streams was assumed to be negligible. For  
207 the same means, the effluent from the conversion stage was recycled back to the ponds instead of  
208 being directly disposed. Considering the above assumptions, algal cultivation does not generate a  
209 gray WF and the analysis focused on blue and green WFs with a sensitivity to this assumption  
210 explored.

211 The indirect WFs attributed to process consumables were retrieved from different LCA  
212 databases and literature. Water consumption associated with the production of diammonium-  
213 phosphate, ammonia, hydrogen, and natural gas was retrieved from the GREET 2021 model.<sup>28</sup>  
214 The water consumed in electricity generation was determined by expanding the methods  
215 presented in Lee et al.<sup>29</sup> to an eGRID subregion level.<sup>30</sup> More detailed indirect WF calculations  
216 are provided in the SI.

### 217 2.3.2 Available Water Remaining Methodology

218 The Available Water Remaining in the US (AWARE-US) model<sup>31</sup> was used to calculate the  
219 WSF of algal biomass and biofuels based on a monthly analysis that is averaged into seasonal  
220 results. This model defines the WSF as the product of direct freshwater consumption and a  
221 characterization factor (CF). The CF is a water-stress indicator characterizing the water  
222 availability and demand of a given location relative to the water availability of a specific  
223 location.<sup>6,7</sup> The AWARE-US model provides monthly characterization factors for US counties  
224 relative to the US average freshwater availability.<sup>31</sup> The output of the analysis is a monthly WSF  
225 at a county level. The methods used to interpolate model outputs to a county level are described  
226 in the SI.

227        **3. Results and Discussion**

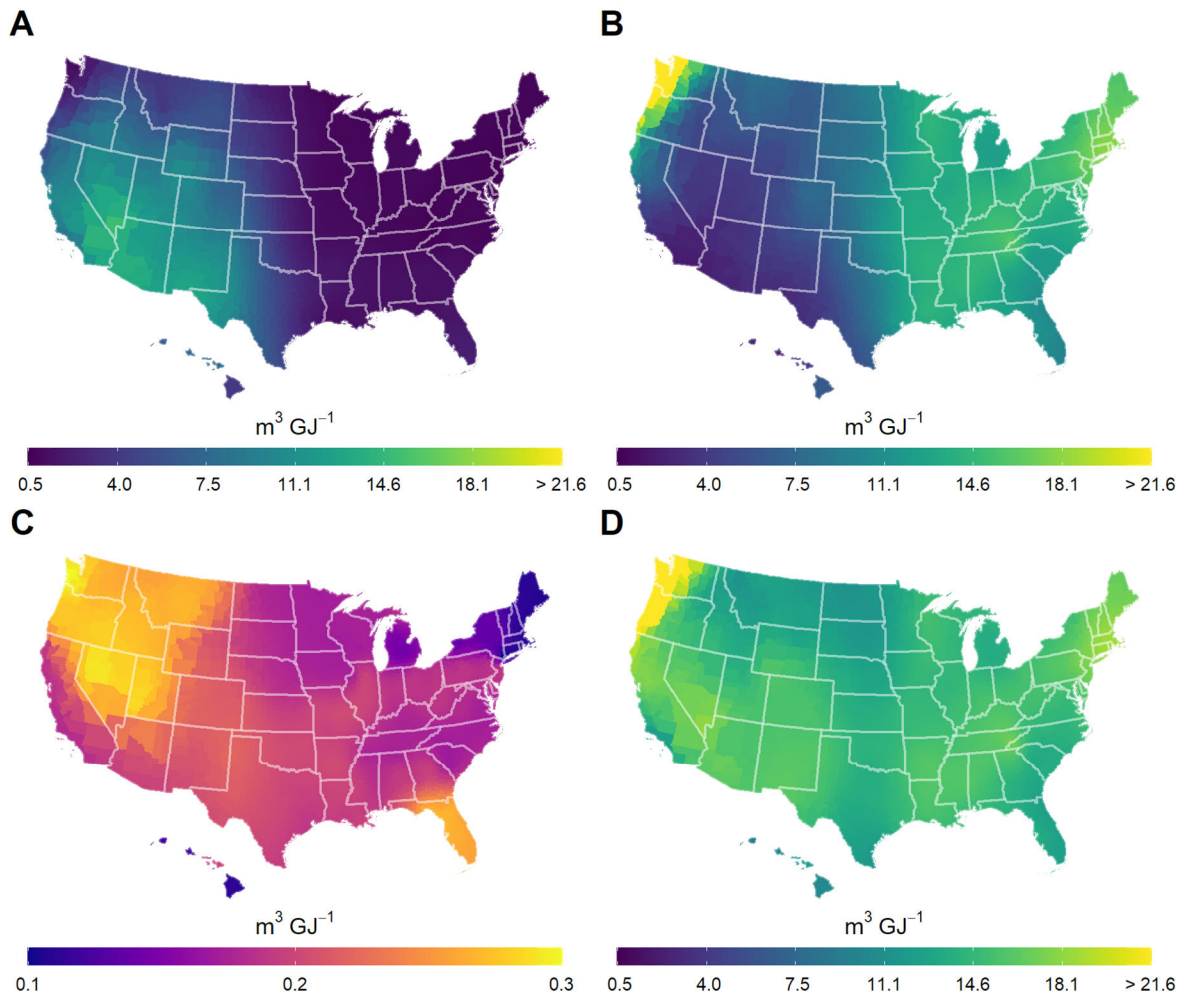
228        The WF of algae biofuels is presented and disaggregated into the direct blue, green, and  
229        indirect blue, and then summed for a total WF. The grey water footprint is regarded as negligible  
230        assuming optimal operation of the system. Process model outputs are then analyzed to  
231        understand the parameters that have a major impact on WF results. Results are combined with  
232        AWARE-CF to determine the WSF of algal-based biofuels with seasonal resolution. The results  
233        presented in this section are the averages of the 21-year simulation.

234        **3.1 National Water Footprint Mapping**

235        The life cycle WF for all simulated sites were surface interpolated and results for the algal  
236        fuels system are summarized in Fig. 2. The range of total life cycle WF was calculated to be 30  
237         $\text{m}^3 \text{ GJ}^{-1}$  with the maximum located in the northwest US ( $39 \text{ m}^3 \text{ GJ}^{-1}$ ), while Hawaii and southern  
238        California yield the smallest WFs, ranging between 9 and  $10.6 \text{ m}^3 \text{ GJ}^{-1}$ . The large WFs in the  
239        Pacific Coast are explained by the high precipitation rates and low biomass yields in the region.  
240        Similarly, the large WF of hydroelectricity has a modest impact on the indirect water  
241        consumption of algae farms located across the northwestern US (Fig. 2C). While the larger  
242        indirect WF of sites in Florida is correlated to the energy penalty associated with elevated  
243        rainwater usage. These results show that even in scenarios with high energy consumption, the  
244        indirect WF is an order of magnitude lower than the direct blue and green components of  
245        freshwater cultivation. In conclusion, direct freshwater and rainwater consumption are the largest  
246        contributors to the total WF and the indirect WF of upstream processes was found to be strongly  
247        dependent on the WF of electricity generation.

248        The results from the work illustrate that the indirect WF of freshwater cultivation is low and  
249        dominated by electricity usage in the system. Contrastingly, the indirect WF is dramatically  
250        impacted in a saline cultivation scenario, where the ~~indirect WF component is particularly~~

251 ~~relevant to saline cultivation, where freshwater is mostly consumed upstream and there is an~~  
252 increase in electricity consumption due to higher pumping and blowdown energy needed to  
253 maintain adequate salinity levels. The differences in WFs between freshwater and saline  
254 cultivation scenarios for Tampa, FL, and Corpus Christi, TX were quantified following the saline  
255 modeling assumptions provided in the SI. Results show that saline cultivation in Corpus Christi,  
256 TX provides a 30% reduction in the total WF by eliminating freshwater consumption to make up  
257 for evaporation which exceeds the increased indirect water consumption from pumping (Fig  
258 S13). In Tampa, FL saline cultivation increased the indirect WF component by an order of  
259 magnitude, which resulted in similar total WFs as the freshwater cultivation scenario. These two  
260 case studies highlight the potential of coastal areas for reducing the WFs of algal systems  
261 through saline cultivation, but also show it is location-dependent.



262

263 **Figure 2.** Life cycle water footprint breakdown of algal diesel: (A) direct blue water footprint, (B)  
 264 direct green water footprint, (C) indirect blue water footprint, and (D) total water footprint.

265 The regional differences observed in Fig. 2 emphasize the need for water LCAs with  
 266 geospatial resolution. For instance, the blue WF (Fig 2A) is driven purely by evaporation rates  
 267 with the highest rates located in dry climates such as the Desert Southwest. Contrastingly, the  
 268 southeastern US shows the largest green WFs (Fig 2B) and the smallest blue WFs, explained by  
 269 the high precipitation rates in the region. However, when comparing the total WF of these  
 270 regions, similar trends are observed in total WFs. For example, the total WF of Phoenix, AZ was

271 found to be only 3% larger than that of Macon, GA, although freshwater consumption in Phoenix  
272 represents 85% of the total water consumption compared to 14% in Macon, GA. The freshwater  
273 consumption in a water-scarce region such as the southwestern US will potentially bring about  
274 more severe environmental impacts than the consumption of rainwater in Georgia. This  
275 comparison stresses a limitation of the water footprint method, as it only accounts for water  
276 consumption, but does not consider water stress impacts. This is further explored in this study  
277 through water scarcity calculations.

278 The results from this study were also compared to published water LCAs using identical  
279 system boundaries and metrics. Compared to the algal WFs ( $m^3 GJ^{-1}$ ) reported by Ou et al.<sup>32</sup>, an  
280 average difference of 14% across the eight sites used for comparison was estimated. These  
281 discrepancies were larger in sites located in the Midwest US and are attributed to differences in  
282 evaporation modeling, meteorological data, and biomass yields. At the same time, the model  
283 used in this study predicts lower freshwater consumption per area ( $m^3 m^{-2} yr^{-1}$ ) across the eight  
284 sites used for comparison, corresponding to an average difference of 38%. Moreover, the  
285 magnitudes of other water consumption sources (i.e. conversion and indirect) agree with the  
286 results from this analysis, implying that differences between water LCAs of algae systems are  
287 mainly attributed to variations in net evaporation rates and growth rates.

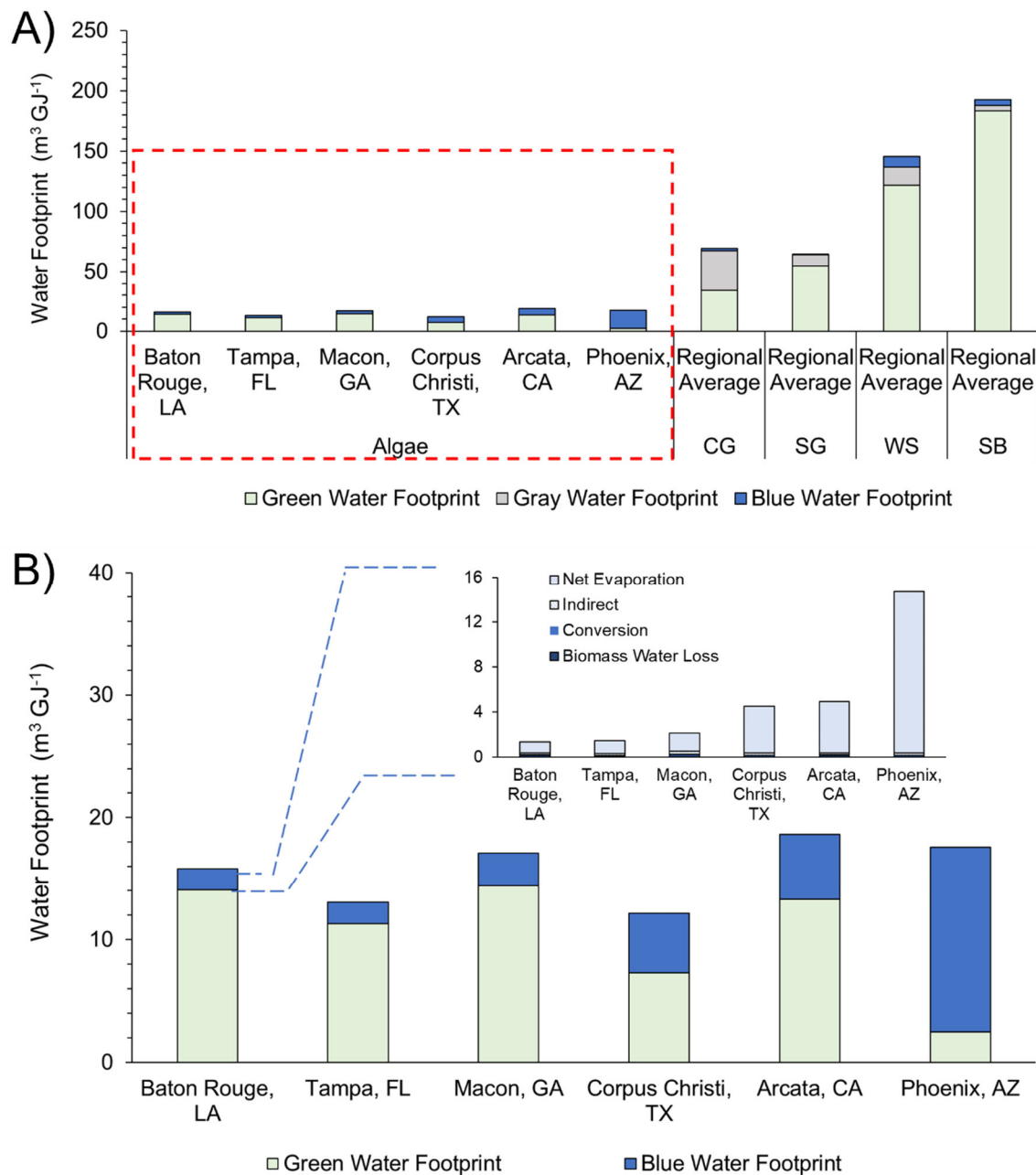
288 Furthermore, a WF comparison to first and second-generation biofuels shows blue WFs of  
289 algal fuel systems can approximate those of conventional corn ethanol and soybean biodiesel  
290 systems, and the difference depends on the location where algal biomass is cultivated. In  
291 particular, the blue WF of algal fuels in the southwestern US is generally larger than the average  
292 blue WFs of corn ethanol and soybean biodiesel cultivated in Iowa, but comparable if algal  
293 biomass is cultivated in the Gulf Coast region (Fig. 3A). A comparison to wheat straw ethanol

294 shows that algal production in California and Texas incurs smaller blue WFs; however, when  
295 algal biomass is cultivated in Arizona, production of first and second-generation biofuels  
296 generates a smaller blue WF. Although a larger volume of freshwater is required for algal  
297 cultivation in these locations, the higher biomass yields make the blue WF of algal biofuels  
298 comparable to those of its first and second-generation counterparts. In summary, the regional  
299 variations of freshwater consumption and biomass yields must be considered to determine the  
300 scenarios under which algal fuels present a smaller blue WF than conventional biofuel systems.

301 In the context of the green WF component, algal systems present some advantages over  
302 terrestrial energy crops. Notably, the impact of higher growth rates achieved by algae systems is  
303 best reflected when comparing the green WF between biofuels. The results illustrated in Fig. 3A  
304 show that algal renewable diesel uses less rainwater per unit of energy than all other biofuel  
305 systems.

306 In terms of gray water, algal cultivation presents the advantage of generating no gray WF if  
307 pollutants loadings in waste streams are carefully tracked, ponds are properly managed, and  
308 recycling across process stages is practiced.<sup>16,33</sup> It is important to note that complete nutrient  
309 assimilation in the ponds is critical for maintaining negligible gray WFs in algae systems.  
310 Negligible gray WFs in algal systems are dependent on proper pond management, and operating  
311 the ponds without carefully tracking nutrient loadings and water discharged volumes could result  
312 in considerable gray WFs (Fig. S2). Contrastingly, the gray WF of terrestrial crops is a function  
313 of fertilizer loss and has been found to represent a large portion of the total WF<sup>34,35</sup>, particularly  
314 for corn ethanol (Fig. 3A). Based on the modeled gray WFs, findings of this comparison suggest  
315 that a shift to algal biofuels has the potential to lower the gray and green water consumption of  
316 bioenergy.

317 As shown in Fig. 3A, if all components are considered, the total WF of algal biofuel systems is  
318 approximately four to six times smaller than the average WF of corn ethanol while an order of  
319 magnitude smaller than that of soybean biodiesel. If only blue and gray WFs are compared, algal  
320 systems have a larger total WF than soybean and switchgrass biofuels but a smaller total WF  
321 than corn grain and wheat straw ethanol. This comparison indicates that from an overall WF  
322 perspective, algal systems benefit from their higher growth rates and opportunity for recycling  
323 nutrients.



324

325 **Figure 3. A)** Life cycle water footprint comparison between renewable diesel from microalgal  
 326 biomass for six locations in the United States and average regional life cycle water footprints for  
 327 first and second-generation biofuels derived from corn grain (CG), switchgrass (SG), wheat straw  
 328 (WS), and soybean (SB). The water footprints of corn grain and wheat straw ethanol, as well as  
 329 those of soybean biodiesel and switchgrass biodiesel blend, were retrieved from the literature<sup>36-39</sup>

330 and represent average values of high crop production areas: corn and soybean are assumed to be  
331 grown in the Corn Belt and the southeastern US, while switchgrass and wheat straw are mainly  
332 cultivated in the central and eastern US. B) Life cycle water footprint of algal fuel systems across  
333 six locations in the US. Inset, the blue water footprint breakdown. The water footprint values of  
334 algae sites represent the average of the 21 simulated years.

335

### 336 3.2 Water Footprint Breakdown

337 The results shown are all driven by the different parameters calculated by the engineering  
338 process model, thus, evaluating the mass and energy balance is critical to identifying  
339 opportunities for reducing freshwater consumption. The analysis indicates that freshwater and  
340 rainwater consumption in the biomass production process dominates the overall water  
341 consumption of algae systems. As seen in the blue WF breakdown of the six case study locations  
342 shown in Fig. 3B, water consumed in the conversion process is minimal compared to the  
343 evaporation losses during the cultivation stage. Consequently, algae fuel systems benefit from  
344 the recycling of cultivation water embedded in the biomass making them less water-intensive  
345 than traditional terrestrial-based biomass systems, where the water leaving with the biomass is  
346 assumed to be consumed. The outcomes from both modeled system boundaries demonstrate that  
347 water consumed in the biomass production stage dominates the total WF and the co-location of  
348 biorefineries with farms decreases the WF of algae fuels by promoting water recycling across  
349 processes.

350 Beyond the effects of water recycling, the usage of rainwater also contributes to minimizing  
351 freshwater withdrawal and consumption. This is observed when comparing the net evaporation  
352 rates in this study, ranging from  $0.05$  to  $1.47 \text{ m}^3 \text{ m}^{-2} \text{ yr}^{-1}$ , with the range previously calculated by  
353 Quiroz et al.<sup>11</sup> ( $0.30$ - $1.68 \text{ m}^3 \text{ m}^{-2} \text{ yr}^{-1}$ ). The wider range presented in Quiroz et al.<sup>11</sup> is expected,

354 as rainwater was not accounted for, and instead, a “gross” evaporation rate was estimated. The  
355 southeastern US is one of the regions that benefit the most from rainfall utilization. For example,  
356 in Tampa, FL most of the water consumption can be supplied with rainwater. The model outputs  
357 demonstrate that the net water consumption of algal systems is primarily influenced by  
358 evaporation losses and rainwater contributes to increasing the water efficiency of these systems.

359 The evaporation losses in the cultivation stage drive the water intensity of algal systems  
360 therefore it is critical to select sound evaporation models to reduce the uncertainty in evaporation  
361 estimates. To understand the importance of evaporation modeling in water usage metrics, net  
362 evaporation rates were compared to those of Wigmosta et al.<sup>17</sup> In general, the results from this  
363 study were found to be 31% lower, based on the 204 sites used for comparison. This difference is  
364 anticipated as Wigmosta et al.<sup>17</sup> used corrected pan evaporation data for model validation<sup>17</sup>,  
365 which has been shown to differ by 45% from commercial-scale algae systems.<sup>11</sup> The differences  
366 in scales of the modeled facilities are critical as the surface area has a direct influence on  
367 evaporation rates.<sup>11</sup> Facility sizes modeled in Wigmosta et al.<sup>17</sup> were selected based on land  
368 availability, while this work fixed a standard 400-ha wetted area. Although direct comparison  
369 would require harmonizing model inputs, the comparison highlights the importance of selecting  
370 appropriate evaporation models when modeling water consumption in open algae systems

371 Biomass yields have a direct impact on the WF of the system, as it impacts the functional unit.  
372 The modeled productivity yields agree with experimental values for UTEX 393<sup>23</sup> with annual  
373 averages ~~areal productivity reached~~ reaching a maximum of  $23.6 \text{ g m}^{-2} \text{ day}^{-1}$  in Hawaii and  
374 Florida (Fig S4A). It should be noted that these values represent optimistic yields for commercial  
375 microalgae cultivation since the impacts of culture failure are not accounted for in the analysis.  
376 The potential impacts of pond contamination on modeled areal productivity values are illustrated

377 by reducing biomass yields by a safety factor (Fig S5). The results presented here represent  
378 projections based on the current biomass production potential in pilot-scale systems and should  
379 be improved by considering the impacts of culture mixing in commercial-scale systems as well  
380 as pond contamination and reliability.

381 Other model outputs were found to be consistent with previous modeling work.<sup>11</sup> Nutrient  
382 demands were found to scale directly with biomass yields, while electricity consumption is a  
383 function of operational days, growth rates, and precipitation rates (Fig. S6). The high electricity  
384 demand in the Gulf Coast states is credited to the higher pumping and dewatering power needed  
385 to control the depth of the ponds during periods of intense rainfall. Energy balance results show  
386 that minimizing freshwater use through the effective use of rainwater in the cultivation process  
387 comes with an increase in electricity consumption caused by more frequent pond harvesting and  
388 larger processing volumes.

389 Moreover, the impacts of model inputs on the blue and indirect WFs for two case study  
390 locations were tested through a sensitivity analysis (details included in the SI). The results of the  
391 sensitivity analysis (Fig. S16) indicate that in sites with low precipitation such as Phoenix, AZ  
392 the parameters that directly impact evaporation losses and biomass yields are the most sensitive  
393 to both the direct blue water footprint and indirect water footprint. Contrastingly, in sites with  
394 high precipitation such as Tampa, FL, the depth limits of the ponds were found to be sensitive.  
395 These inputs have an impact on the amount of rainwater that can be stored in the ponds and  
396 consequently impact the amount of freshwater needed to refill the ponds at the minimum depth.  
397 Although a reduction in the separation efficiency reduces the amount of biomass converted into  
398 fuels, there is also a decrease in the amount of water needed to make up for losses, as more water  
399 is recycled back to the ponds. An increase in the separation efficiency increases the amount of

400 biomass that is sent to conversion but increases the volume of water needed to make up for water  
401 losses (less water is recycled) and therefore balances the impacts of increased yields on the blue  
402 water footprint of the system.

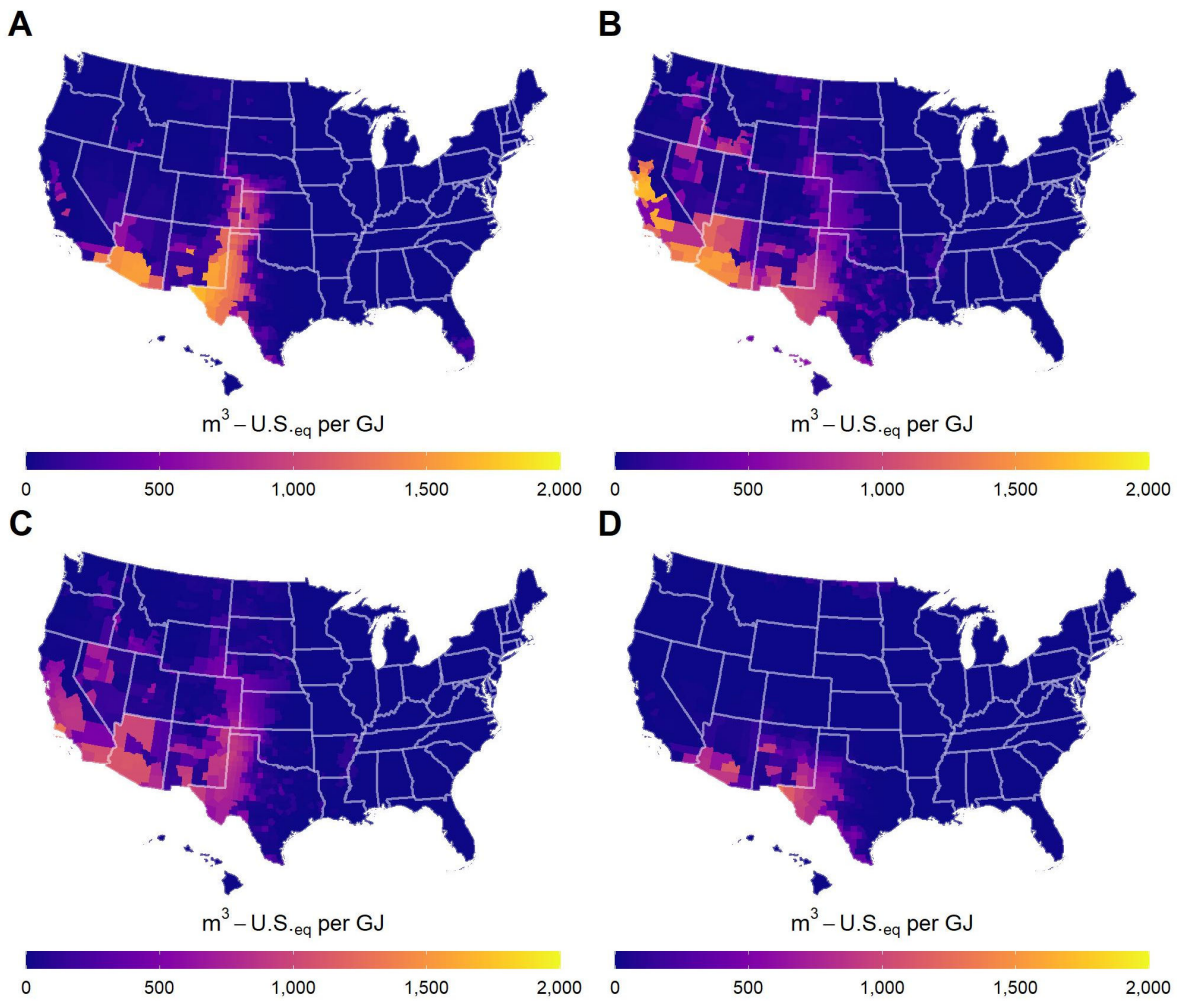
403 **3.3 Water Scarcity Implications**

404 Aside from quantifying life cycle water usage, the local water stress associated with the  
405 deployment of algal systems was calculated and reported as a WSF. The seasonal results shown  
406 in Fig. 4 illustrate the temporal dynamics of water consumption, availability, and biomass yields.  
407 The largest WSFs are found in the southwestern US, where water stress levels vary between  
408 1700 and 1760 m<sup>3</sup>-U.S.<sub>eq</sub> per GJ during spring (Fig 4A). Similar water stress levels propagate to  
409 southern and western California during the summer (Fig 4B). While there is an increase in water  
410 consumption during summer, this is balanced by an increase in biomass yields, consequently, the  
411 magnitude of WSFs during summer is comparable to those seen in spring. Similarly, the same  
412 regions present the highest water stress levels during the fall season (Fig 4C), but there is a  
413 reduction in the WSF compared to summer levels. The winter season experiences a reduction in  
414 water stress levels in California while southwestern Texas displays a minor change compared to  
415 fall. The seasonal analysis indicates that biomass yields drive the WSF during spring and  
416 summer, while water consumption is the driving factor during the fall and winter seasons.

417 As discussed above, the temporal variations of the WSF are a product of the seasonal  
418 variabilities of freshwater consumption and biomass yields. Potential algae sites must support  
419 high growth and low evaporation rates, in addition, sites must be located in areas with sufficient  
420 water availability to support a low WSF (low AWARE-US CF). Based on these criteria, the  
421 southeastern and Gulf Coast U.S are characterized as the most suitable regions for microalgal  
422 fuels (Fig. 4) and biomass production considering WSF (Fig. S14). The southeastern US region  
423 achieves the maximum biomass yields with average areal productivities above 20 g m<sup>-2</sup> day<sup>-1</sup> and

424 the abundant rainwater has a propitious effect on the WSF, by not only reducing the water  
425 consumption of algal systems but also increasing freshwater availability and therefore returning a  
426 low AWARE-US CF. There was found to be minimal variability among the distribution of WSF  
427 for counties in Gulf Coast states and Georgia. Even in the scenario of having below-average  
428 precipitation rates, the maximum seasonal WSF in the region remains between 5.2 and 5.8 m<sup>3</sup>-  
429 U.S.<sub>eq</sub> m<sup>-2</sup> month<sup>-1</sup>, suggesting that the WSF is more strongly correlated to biomass yields. The  
430 analysis reveals that the southeastern US is the best candidate for siting algal systems based on  
431 WSF due to the low water consumption, high growth rates, and low water stress levels.

432



433

434 **Figure 4.** Seasonal water scarcity footprints of renewable diesel from algal biomass: (A) spring,  
 435 (B) summer, (C) fall, and (D) winter.

436        Although sites in the southwestern US also present high biomass yields, low water  
 437 availability in the western US risks unsustainable cultivation of algal biomass in the region. For  
 438 instance, if algal farms are projected to be deployed in Arizona or southern California, these  
 439 facilities will need to be supported by saline water sources to avoid any negative water stress  
 440 impacts and minimize freshwater withdrawals. Furthermore, if freshwater were available in the  
 441 region, algal biomass proves to be a more efficient user of water than conventional energy crops

442 and could potentially substitute terrestrial protein crops (e.g., soybean) in water-scarce regions  
443 such as CA and AZ.

444 Moreover, the results presented here suggest that the deployment of algal systems would not  
445 stress water resources in the southeastern US and thus could be developed alongside traditional  
446 agriculture. Although this study is not meant to establish the freshwater, wastewater, or saline  
447 resource availability and the implications on the scalability of these systems, the water scarcity  
448 analysis shows that freshwater consumption should not be a deterrent against the scale-up of  
449 algal facilities in certain geographical locations. However, land and CO<sub>2</sub> availability in the  
450 southeastern US are resources that could risk the sustainable scaling of these systems.<sup>17,40</sup>  
451 Ultimately, freshwater is not a resource limiting the scale-up of algal biomass production and  
452 algal biomass can be characterized as a low water alternative to conventional terrestrial energy  
453 crops.

454 It is also important to note that the WSFs presented here consider only freshwater  
455 consumption impacts. As discussed, the cultivation of algal biomass in the southeastern US will  
456 require an appropriation of the available precipitation that could lead to changes in green water  
457 availability or impact the water supply of other crops in the area. Additionally, freshwater  
458 availability can also be reduced as groundwater will not be naturally recharged by rainwater.<sup>41</sup>  
459 Therefore, expansion of this analysis could investigate the green WSF of algal cultivation in  
460 areas where green water consumption dominates and analyze the tradeoffs between areas with  
461 large blue WSF and those with large green WSF.

462 **4 Conclusions**  
463

464 The WF and WSF of microalgal biomass cultivation and conversion to fuel across the  
465 continental US and Hawaii are evaluated through a regionalized water LCA. The biomass  
466 cultivation stage was found to be the most water-intensive process with evaporation losses in  
467 open ponds representing the major source of freshwater consumption in the system. When all  
468 WF components are considered, the WF of algal renewable diesel was found to be smaller than  
469 that of traditional biofuels, however, algal biofuels generate larger blue WFs. The smaller WFs  
470 of algal renewable diesel are a result of both higher growth rates and the lack of a gray WF  
471 component stemming from nutrient recycling and proper waste stream management. In terms of  
472 WSF, sites in the Gulf Coast and the southeastern US were found to have the lowest water stress  
473 levels. Finally, cultivation in the southwestern US will cause substantial water stress in the  
474 region and saline algal cultivation is advised to reduce the water consumption of sites in these  
475 water-scarce regions. The potential of reducing the WF of algal systems in coastal areas by  
476 implementing saline cultivation was also explored. Although saline cultivation reduces  
477 freshwater consumption, there is an increase in indirect water consumption and future work  
478 should focus on better quantifying this component as it was shown to be equivalent to the water  
479 savings associated with evaporative makeup water. Finally, for a true understanding of the  
480 potential indirect water consumption impacts associated with cultivation in saline or brackish  
481 water, a detailed quantification of the energetics of groundwater pumping and brine disposal  
482 methods is required.

483

484

485

486

487

488 ASSOCIATED CONTENT

489 **Supporting Information.**

490 The following files are available free of charge.

491 Detailed model structure and assumptions, equations used in the water balance calculations,  
492 primary model inputs, life cycle inventory, county-level interpolation methods, additional model  
493 outputs, and additional water footprint and water scarcity footprint results. (. PDF)  
494 County-level water footprints and water scarcity footprints for reproduction of Figure 2 and  
495 Figure 4 (.xlsx)

496

497 AUTHOR INFORMATION

498 **Corresponding Author**

499 David Quiroz – Mechanical Engineering Department, Colorado State University, 1374 Campus  
500 Delivery, Fort Collins, Colorado 80522, United States

501 \* E-mail: david.quiroz\_nuila@colostate.edu

502 **Author Contributions**

503 The manuscript was written through the contributions of all authors. All authors have given  
504 approval to the final version of the manuscript.

505 **Funding Sources**

506 The authors acknowledge funding support from the DOE grant DE-EE0008906.

507 **Notes**

508 Any additional relevant notes should be placed here.

509 ACKNOWLEDGMENT

510 The authors would like to thank the members of the Quinn Lab Group for their support and  
511 insights. The authors would like to acknowledge Peter Chen for sharing his discussions on the  
512 topic. The authors express their gratitude to John McGowen from the Arizona Center for Algae  
513 Technology and Innovation for the valuable discussions on the topic. The authors gratefully  
514 acknowledge Danna Quinn for editing.

515 ABBREVIATIONS

516 AWARE, Available Water Remaining; CF, characterization factor; eGRID, Emissions and  
517 Generation Resource Integrated Database; GREET, Greenhouse Gases, Regulated Emissions,  
518 and Energy Use in Technologies Model; HTL, hydrothermal liquefaction; LCA, life-cycle  
519 assessment; ORP, open-raceway pond; US, United States; WF, water footprint; WSF, water  
520 scarcity footprint; WULCA, Water Use in LCA.

521

522

523

524

525

526

527 REFERENCES

528 (1) Wijffels, R. H.; Barbosa, M. J. An Outlook on Microalgal Biofuels. *Science (1979)*  
529 **2010**, 329 (5993), 796–799. <https://doi.org/10.1126/SCIENCE.1189003>.

530 (2) Kumar, B. R.; Mathimani, T.; Sudhakar, M. P.; Rajendran, K.; Nizami, A. S.;  
531 Brindhadevi, K.; Pugazhendhi, A. A State of the Art Review on the Cultivation of Algae  
532 for Energy and Other Valuable Products: Application, Challenges, and Opportunities.  
533 *Renewable and Sustainable Energy Reviews*. Elsevier Ltd March 1, 2021, p 110649.  
534 <https://doi.org/10.1016/j.rser.2020.110649>.

535 (3) Cruce, J. R.; Beattie, A.; Chen, P.; Quiroz, D.; Somers, M.; Compton, S.; DeRose,  
536 K.; Beckstrom, B.; Quinn, J. C. Driving toward Sustainable Algal Fuels: A Harmonization  
537 of Techno-Economic and Life Cycle Assessments. *Algal Research*. Elsevier B.V. April 1,  
538 2021, p 102169. <https://doi.org/10.1016/j.algal.2020.102169>.

539 (4) Williams, A. P.; Cook, E. R.; Smerdon, J. E.; Cook, B. I.; Abatzoglou, J. T.; Bolles,  
540 K.; Baek, S. H.; Badger, A. M.; Livneh, B. Large Contribution from Anthropogenic  
541 Warming to an Emerging North American Megadrought. *Science (1979)* **2020**, 368 (6488),  
542 314–318.  
543 [https://doi.org/10.1126/SCIENCE.AAZ9600/SUPPL\\_FILE/AAZ9600\\_WILLIAMS\\_SM.PDF](https://doi.org/10.1126/SCIENCE.AAZ9600/SUPPL_FILE/AAZ9600_WILLIAMS_SM.PDF).

545 (5) Hoekstra, A. Y.; Chapagain, A. K.; Aldaya, M. M.; Mekonnen, M. M. *The Water  
546 Footprint Assessment Manual*; Earthscan: London, 2011.

547 (6) Boulay, A. M.; Bare, J.; De Camillis, C.; Döll, P.; Gassert, F.; Gerten, D.; Humbert,  
548 S.; Inaba, A.; Itsubo, N.; Lemoine, Y.; Margni, M.; Motoshita, M.; Núñez, M.; Pastor, A.

549 V.; Ridoutt, B.; Schencker, U.; Shirakawa, N.; Vionnet, S.; Worbe, S.; Yoshikawa, S.;  
550 Pfister, S. Consensus Building on the Development of a Stress-Based Indicator for LCA-  
551 Based Impact Assessment of Water Consumption: Outcome of the Expert Workshops.  
552 *International Journal of Life Cycle Assessment* **2015**, *20* (5), 577–583.  
553 <https://doi.org/10.1007/S11367-015-0869-8/FIGURES/1>.

554 (7) Boulay, A. M.; Bare, J.; Benini, L.; Berger, M.; Lathuillière, M. J.; Manzardo, A.;  
555 Margni, M.; Motoshita, M.; Núñez, M.; Pastor, A. V.; Ridoutt, B.; Oki, T.; Worbe, S.;  
556 Pfister, S. The WULCA Consensus Characterization Model for Water Scarcity Footprints:  
557 Assessing Impacts of Water Consumption Based on Available Water Remaining  
558 (AWARE). *International Journal of Life Cycle Assessment* **2018**, *23* (2), 368–378.  
559 <https://doi.org/10.1007/S11367-017-1333-8/FIGURES/2>.

560 (8) Guiyesse, B.; Béchet, Q.; Shilton, A. Variability and Uncertainty in Water Demand  
561 and Water Footprint Assessments of Fresh Algae Cultivation Based on Case Studies from  
562 Five Climatic Regions. *Bioresource Technology* **2013**, *128*, 317–323.  
563 <https://doi.org/10.1016/j.biortech.2012.10.096>.

564 (9) Batan, L.; Quinn, J. C.; Bradley, T. H. Analysis of Water Footprint of a  
565 Photobioreactor Microalgae Biofuel Production System from Blue, Green and Lifecycle  
566 Perspectives. *Algal Research* **2013**, *2* (3), 196–203.  
567 <https://doi.org/10.1016/J.ALGAL.2013.02.003>.

568 (10) Clarens, A. F.; Resurreccion, E. P.; White, M. A.; Colosi, L. M. Environmental Life  
569 Cycle Comparison of Algae to Other Bioenergy Feedstocks. *Environmental Science and  
570 Technology* **2010**, *44* (5), 1813–1819. <https://doi.org/10.1021/es902838n>.

571 (11) Quiroz, D.; Greene, J. M.; McGowen, J.; Quinn, J. C. Geographical Assessment of  
572 Open Pond Algal Productivity and Evaporation Losses across the United States. *Algal*  
573 *Research* **2021**, *60*, 102483. <https://doi.org/10.1016/J.ALGAL.2021.102483>.

574 (12) Gerbens-Leenes, P. W.; Xu, L.; de Vries, G. J.; Hoekstra, A. Y. The Blue Water  
575 Footprint and Land Use of Biofuels from Algae. *Water Resources Research* **2014**, *50* (11),  
576 8549–8563. <https://doi.org/10.1002/2014WR015710>.

577 (13) Yang, J.; Xu, M.; Zhang, X.; Hu, Q.; Sommerfeld, M.; Chen, Y. Life-Cycle  
578 Analysis on Biodiesel Production from Microalgae: Water Footprint and Nutrients Balance.  
579 *Bioresource Technology* **2011**, *102* (1), 159–165.  
580 <https://doi.org/10.1016/j.biortech.2010.07.017>.

581 (14) Xu, H.; Lee, U.; Coleman, A. M.; Wigmosta, M. S.; Wang, M. Assessment of Algal  
582 Biofuel Resource Potential in the United States with Consideration of Regional Water  
583 Stress. *Algal Research* **2019**, *37*, 30–39. <https://doi.org/10.1016/J.ALGAL.2018.11.002>.

584 (15) Xu, H.; Lee, U.; Coleman, A. M.; Wigmosta, M. S.; Sun, N.; Hawkins, T.; Wang,  
585 M. Balancing Water Sustainability and Productivity Objectives in Microalgae Cultivation:  
586 Siting Open Ponds by Considering Seasonal Water-Stress Impact Using AWARE-US.  
587 *Environmental Science and Technology* **2020**, *54* (4), 2091–2102.  
588 [https://doi.org/10.1021/ACS.EST.9B05347/SUPPL\\_FILE/ES9B05347\\_SI\\_001.PDF](https://doi.org/10.1021/ACS.EST.9B05347/SUPPL_FILE/ES9B05347_SI_001.PDF).

589 (16) Gerbens-Leenes, P. W.; Xu, L.; de Vries, G. J.; Hoekstra, A. Y. The Blue Water  
590 Footprint and Land Use of Biofuels from Algae. *Water Resources Research* **2014**, *50* (11),  
591 8549–8563. <https://doi.org/10.1002/2014WR015710>.

592 (17) Wigmosta, M. S.; Coleman, A. M.; Skaggs, R. J.; Huesemann, M. H.; Lane, L. J.  
593 National Microalgae Biofuel Production Potential and Resource Demand. *Water Resources*  
594 *Research* **2011**, *47* (4), 1–13. <https://doi.org/10.1029/2010WR009966>.

595 (18) Frank, Edward D., Han, J., Palou-Rivera, I., Elgowainy, A., Wang, M. Q. *Life-*  
596 *Cycle Analysis of Algal Lipid Fuels with the GREET Model*; 2011.

597 (19) Chen, P. H.; Quinn, J. C. Microalgae to Biofuels through Hydrothermal  
598 Liquefaction: Open-Source Techno-Economic Analysis and Life Cycle Assessment.  
599 *Applied Energy* **2021**, *289*, 116613. <https://doi.org/10.1016/J.APENERGY.2021.116613>.

600 (20) Greene, J. M.; Quiroz, D.; Compton, S.; Lammers, P. J.; Quinn, J. C. A Validated  
601 Thermal and Biological Model for Predicting Algal Productivity in Large Scale Outdoor  
602 Cultivation Systems. *Algal Research* **2021**, *54*, 102224.  
603 <https://doi.org/10.1016/j.algal.2021.102224>.

604 (21) Nguyen, P.; Shearer, E. J.; Tran, H.; Ombadi, M.; Hayatbini, N.; Palacios, T.;  
605 Huynh, P.; Braithwaite, D.; Updegraff, G.; Hsu, K.; Kuligowski, B.; Logan, W. S.;  
606 Sorooshian, S. The CHRS Data Portal, an Easily Accessible Public Repository for  
607 PERSIANN Global Satellite Precipitation Data. *Scientific Data* **2019** *6*:1 **2019**, *6* (1), 1–10.  
608 <https://doi.org/10.1038/sdata.2018.296>.

609 (22) Davis, R.; Markham, J.; Kinchin, C.; Grundl, N.; Tan, E.; Humbird, D. Process  
610 Design and Economics for the Production of Algal Biomass: Algal Biomass Production in  
611 Open Pond Systems and Processing Through Dewatering for Downstream Conversion.  
612 *National Renewable Energy Laboratory* **2016**, No. February, 128.

613 (23) Davis, R.; Laurens, L. Algal Biomass Production via Open Pond Algae Farm  
614 Cultivation: 2019 State of Technology and Future Research. **2020**, No. April, 1–32.

615 (24) Zhang, B.; Ogden, K. Nitrogen Balances and Impacts on the Algae Cultivation-  
616 Extraction-Digestion-Cultivation Process. *Algal Research* **2019**, *39*, 101434.  
617 <https://doi.org/10.1016/J.AL GAL.2019.101434>.

618 (25) Griffiths, M. J.; van Hille, R. P.; Harrison, S. T. L. The Effect of Nitrogen  
619 Limitation on Lipid Productivity and Cell Composition in Chlorella Vulgaris. *Applied*  
620 *Microbiology and Biotechnology* **2014**, *98* (5), 2345–2356. <https://doi.org/10.1007/S00253-013-5442-4/TABLES/2>.

622 (26) Ikaran, Z.; Suárez-Alvarez, S.; Urreta, I.; Castañón, S. The Effect of Nitrogen  
623 Limitation on the Physiology and Metabolism of Chlorella Vulgaris Var L3. *Algal Research*  
624 **2015**, *10*, 134–144. <https://doi.org/10.1016/J.AL GAL.2015.04.023>.

625 (27) Fagerstone, K. D.; Quinn, J. C.; Bradley, T. H.; de Long, S. K.; Marchese, A. J.  
626 Quantitative Measurement of Direct Nitrous Oxide Emissions from Microalgae Cultivation.  
627 *Environmental Science and Technology* **2011**, *45* (21), 9449–9456.  
628 [https://doi.org/10.1021/ES202573F/SUPPL\\_FILE/ES202573F\\_SI\\_001.PDF](https://doi.org/10.1021/ES202573F/SUPPL_FILE/ES202573F_SI_001.PDF).

629 (28) GREET. GREET Life Cycle Model User Guide. *Argonne National Laboratory*  
630 **2020**, 169–232.

631 (29) Lee, U.; Chou, J.; Xu, H.; Carlson, D.; Venkatesh, A.; Shuster, E.; Skone, T. J.;  
632 Wang, M. Regional and Seasonal Water Stress Analysis of United States Thermoelectricity.

633 *Journal of Cleaner Production* 2020, 270, 122234.  
634 [https://doi.org/10.1016/j.jclepro.2020.122234.](https://doi.org/10.1016/j.jclepro.2020.122234)

635 (30) United States Environmental Protection Agency (EPA). 2022. "Emissions &  
636 Generation Resource Integrated Database (eGRID), 2020" Washington, DC: Office of  
637 Atmospheric Programs, Clean Air Markets Division. Available from EPA's eGRID web  
638 site: <https://www.epa.gov/egrid>

639 (31) Lee, U.; Xu, H.; Daystar, J.; Elgowainy, A.; Wang, M. AWARE-US: Quantifying  
640 Water Stress Impacts of Energy Systems in the United States. *Science of the Total  
641 Environment* **2019**, *648*, 1313–1322. <https://doi.org/10.1016/j.scitotenv.2018.08.250>.

642 (32) Ou, L.; Banerjee, S.; Xu, H.; Coleman, A. M.; Cai, H.; Lee, U.; Wigmosta, M. S.;  
643 Hawkins, T. R. Utilizing High-Purity Carbon Dioxide Sources for Algae Cultivation and  
644 Biofuel Production in the United States: Opportunities and Challenges. *Journal of Cleaner  
645 Production* **2021**, *321*, 128779. <https://doi.org/10.1016/J.JCLEPRO.2021.128779>.

(33) Farooq, W.; Suh, W. I.; Park, M. S.; Yang, J. W. Water Use and Its Recycling in Microalgae Cultivation for Biofuel Application. *Bioresource Technology* **2015**, *184*, 73–81.  
<https://doi.org/10.1016/J.BIOTECH.2014.10.140>.

649 (34) Chiu, Y. W.; Wu, M. Assessing County-Level Water Footprints of Different  
650 Cellulosic-Biofuel Feedstock Pathways. *Environmental Science and Technology* **2012**, *46*  
651 (16), 9155–9162.  
652 [https://doi.org/10.1021/ES3002162/SUPPL\\_FILE/ES3002162\\_SI\\_001.PDF](https://doi.org/10.1021/ES3002162/SUPPL_FILE/ES3002162_SI_001.PDF).

653 (35) Wu, M.; Chiu, Y.; Demissie, Y. Quantifying the Regional Water Footprint of  
654 Biofuel Production by Incorporating Hydrologic Modeling. *Water Resources Research*  
655 2012, 48 (10), 10518. <https://doi.org/10.1029/2011WR011809>.

656 (36) Argonne National Laboratory. (2013) Water Analysis Tool for Energy Resources  
657 (WATER), “Corn Grain-Grain, Fermentation, Dry milling,” Available from  
658 <http://www.water.es.anl.gov>

659 (37) Argonne National Laboratory. (2013) Water Analysis Tool for Energy Resources  
660 (WATER), “Wheat Straw, Wheat Straw-to-Ethanol, Bioelectricity,” Available from  
661 <http://www.water.es.anl.gov>

662 (38) Argonne National Laboratory. (2013) Water Analysis Tool for Energy Resources  
663 (WATER), “Soybean, Soybean-to-Biodiesel,” Available from <http://www.water.es.anl.gov>

664 (39) Argonne National Laboratory. (2013) Water Analysis Tool for Energy Resources  
665 (WATER), “Switchgrass, Perennial Grass-to-Renewable Biodiesel Blend, Biochemical”,  
666 Available from <http://www.water.es.anl.gov>

667 (40) Quinn, J. C.; Catton, K. B.; Johnson, S.; Bradley, T. H. Geographical Assessment  
668 of Microalgae Biofuels Potential Incorporating Resource Availability. *Bioenergy Research*  
669 2013, 6 (2), 591–600. <https://doi.org/10.1007/S12155-012-9277-0/TABLES/2>.

670 (41) Xu, H.; Wu, M. A First Estimation of County-Based Green Water Availability and  
671 Its Implications for Agriculture and Bioenergy Production in the United States. *Water 2018,*  
672 *Vol. 10, Page 148 2018, 10 (2), 148.* <https://doi.org/10.3390/W10020148>.

673